

Development and Evaluation of Chitosan-Coated PLGA Nanoparticles of Canagliflozin for the Treatment of Hepatic Cancer

Shadab Md^{1,*}, Eman Abdulmoen Abdullah Alharthi¹, Shahid Karim²

¹Department of Pharmaceutics, Faculty of Pharmacy, King Abdulaziz University, Jeddah, SAUDI ARABIA.

²Department of Clinical Pharmacology, Faculty of Medicine, King Abdulaziz University, Jeddah, SAUDI ARABIA.

ABSTRACT

Aim: The aim of the study was to develop, optimize and evaluate chitosan-coated Poly (Lactic-Co-Glycolic Acid) (PLGA) Nanoparticles (NPs) of Canagliflozin (CFZ) against the proliferation of liver cancer cells. **Materials and Methods:** The PLGA NPs and chitosan-coated PLGA NPs containing CFZ was optimized keeping CFZ:PLGA ratios and PVA levels as independent variables and mean Particle Size (PS), Polydispersity Index (PDI), Zeta Potential (ZP), and percent Entrapment Efficiency (EE) as the responses. **Results:** The optimized CFZ-PLGA-NPs had PS, PDI, ZP, and EE values of 159 nm, 0.149, -36.5 mV, 84.8%, respectively. The concentration of chitosan coating (0.25%) was found to be optimum providing a PS of 277±23 nm, PDI of 0.241±0.011, ZP of 57.2±0.67 mV, and EE of 80.5±1.78%. The electron microscope images, FTIR spectra, and DSC thermograms confirmed the identity of individual components and the amorphous nature of CFZ in the C-CFZ-PLGA-NPs. The *in vitro* CFZ release from C-CFZ-PLGA-NPs (80.9±1.2%) was significantly higher than that from CFZ dispersion (25.9±1.4%) when studied for 48 h. The cell viability assay demonstrated significant enhancement of cytotoxicity of C-CFZ-PLGA-NPs against HepG2 cells compared to pure CFZ treatments. The C-CFZ-PLGA-NPs were found to be stable when tested for storage stability at 4°C for 90 days. PS, PDI, and ZP remained stable during the entire study period. **Conclusion:** C-CFZ-PLGA-NPs can be considered potential candidates for further studies in providing a commercially viable, stable, and effective system for the delivery of CFZ.

Keywords: Canagliflozin, Chitosan, Cytotoxicity, HepG2 Cells, Liver Cancer, Nanoparticles.

Correspondence:

Dr. Shadab Md

Department of Pharmaceutics, Faculty of Pharmacy, King Abdulaziz University, Jeddah-21589, SAUDI ARABIA.
Email: shaque@kau.edu.sa

Received: 18-07-2025;

Revised: 24-09-2025;

Accepted: 03-11-2025.

INTRODUCTION

Poly (Lactic-Co-Glycolic Acid) (PLGA) has the advantages of biodegradability and biocompatibility. This has led to the immense development and evaluation of PLGA-based Nanoparticles (NPs).¹ Because PLGAs demonstrate both passive targeting of tumors and encapsulation and release of drugs, they have been thoroughly explored for anticancer drug delivery.² However, PLGA NPs still face several difficulties with formulation issues related to drug loading and release. The effective development of complicated generic formulations based on PLGA continues to be elusive. Not only is the formulation of these generic drug products difficult, but the manufacturing processes involving PLGA are also challenging, which adds to the complexity of

product development. Depending on the medications and their intended uses, different commercial PLGA formulations have different compositions and features. For generic pharmaceutical companies looking to develop complicated generic products based on PLGA, the unavailability of established official methodologies for release studies is another major barrier.³

However, providing chitosan coating to PLGA NPs enhances their mucoadhesive qualities thereby increasing the drug's bioavailability.⁴ To be more precise on the effect of chitosan coating on PLGA NPs, chitosan coating enhances physical and chemical stability, regulates drug release, enhances adhesion to mucosal surfaces and tissue permeation, diminishes sudden and premature drug release, lowers uptake of PLGA NPs by macrophages, shows bioadhesive characteristics, and avoids burst drug release.⁵ In addition, to these general advantages, chitosan-based systems have shown tumor-targeted systems. Chitosan has been positioned as a viable vehicle for cancer therapy due to its electrostatic interaction with various therapeutic agents and materials and the presence of cationic functional groups. In recent years, it has also demonstrated potential as an immunological adjuvant for cancer vaccines.⁶



DOI: 10.5530/ijper.20263737

Copyright Information :

Copyright Author (s) 2026 Distributed under
Creative Commons CC-BY 4.0

Publishing Partner : Manuscript Technomedia. [www.mstechnomedia.com]

Canagliflozin (CFZ), a drug used against type 2 diabetes is orally active and marks its action by the inhibition of Sodium-Glucose Co-Transporter-2 (SGLT2).⁷ Interestingly, SGLT2 inhibitors have demonstrated many mechanisms of action against cancer, including the induction of instability in the membrane of mitochondria, the inhibition of the β -catenin and PI3K-Akt mechanisms, the enhancement of cell cycle arrest and apoptosis, and the reduction of oxidative phosphorylation. Reported data suggest that using an SGLT2 inhibitor with a traditional chemotherapy regimen may have some benefits.⁸

Therefore, the potentials of SGLT2 inhibition in anticancer effects have been studied in CFZ also. Reduction of tumor cell growth by inhibition of mitochondrial complex-I mediated respiration, enhancement of AMPK activity, inhibition of MAPK and mTOR-p70S6k/4EBP1 pathways, activation of cell cycle checkpoints, inhibition of cell growth partly by HIF-1 α inhibition, inducing PD-L1 degradation, impairment of glutamine-mediated anaplerosis, and suppression of glutamine metabolism are some of the reported mechanisms of anticancer activity of CFZ.⁹⁻¹²

It is noteworthy that CFZ has reported action of attenuation of the proliferation of liver cancer cells mediated by inhibition of glycolytic metabolism and angiogenic activity.¹³ Meanwhile, the blockade of glucose influx-induced β -catenin activation by CFZ also causes suppression of hepatocellular tumors.¹⁴ Meanwhile, NPs have been identified as a promising approach against liver cancer.¹⁵ However, NPs of CFZ against liver cancer have not yet been explored, and there exists a research gap. Furthermore, chitosan-based NPs are found effective against liver cancer cells.¹⁶ Therefore, chitosan-coated CFZ-loaded PLGA NPs against liver cancer was studied. The study involved the formulation and optimization of CFZ-loaded PLGA NPs and further conversion of this optimized formulation to chitosan-coated CFZ-loaded PLGA NPs. Finally, characterization and assessment of the chitosan-coated CFZ-loaded PLGA NPs were carried out. Cell line studies in HepG2 cells were done to confirm the potential formulation against liver cancer.

MATERIALS AND METHODS

Materials

Canagliflozin was procured from Jamjoom Pharmaceuticals, Jeddah, Saudi Arabia as a gift sample. Poly (Lactic-Co-Glycolic Acid) (PLGA), Poly Vinyl Alcohol (PVA), Chitosan and MTT reagent were purchased from Sigma-Aldrich Inc. (St. Louis, MO, USA). Human liver cancer cells (HepG2) were purchased from ATCC, USA. Nutrient-rich medium (DMEM) was purchased from BIS BioTech, Jeddah, Saudi Arabia. 1% penicillin-streptomycin was purchased from MOLEQULE-ON®, Auckland, New Zealand. Fetal bovine serum was purchased from Sigma, St. Louis, MO, USA.

Preparation, optimization and evaluation of canagliflozin-loaded PLGA NPs

Using the nanoprecipitation technique, Canagliflozin (CFZ)-containing Nanoparticles (NPs) were prepared. CFZ and PLGA were combined in weight ratios of 1:1, 2:2, and 1:4 with a total weight of 50 mg. The combination was thoroughly dissolved in 2 mL of acetone by vortexing. A glass syringe was used to gradually add the solution, drop by drop, into a 10 mL Polyvinyl Alcohol (PVA) solution with concentrations of 2.5, 5, and 7.5 mg/mL. After homogenizing the mixture for 15 min at a speed of 25,000 rpm, the liquid was magnetically stirred for 6 h to let the acetone evaporate. To separate the nanoparticles, the dispersion was re-dispersed in water thrice following centrifugation at 25,000 rpm for 45 min at 4°C. The PLGA nanoparticles of CFZ were evaluated for the effect of the drug: polymer ratio and stabilizer concentration. The dependent factors were Particle Size (PS), Polydispersity Index (PDI), Zeta Potential (ZP), and percent Entrapment Efficiency (EE).

Particle size, Polydispersity Index (PDI) and Zeta Potential (ZP)

PS and PDI were assessed using a Zetasizer Nano ZS from Malvern Instruments, Worcestershire, UK. In this analysis, samples were diluted 50 times and 1.5 mL of the diluted solution was used. ZP measurements were conducted on the samples diluted 20 times and analyzed using a Zetasizer.

Percent Entrapment Efficiency (EE)

The EE of nanoparticles was measured by dissolving weighed amount of nanoparticles in methanol and ultracentrifuging (25°C) for 30 min. Then CFZ was analyzed in the supernatant at 292 nm by UV-vis spectrophotometry. The EE was calculated by comparing the initial drug amount with the amount remaining in the nanoparticles after separation.

Formulation, optimization and evaluation of chitosan-coated PLGA NPs of canagliflozin

In summary, a Polyvinyl Alcohol (PVA) solution (5 mg/mL) was mixed with three different chitosan concentrations (0.25%, 0.5%, and 0.75%) in 0.5% glacial acetic acid. This chitosan-mixed PVA solution (10 mL) was then combined with a Canagliflozin (CFZ) acetone solution at a CFZ to PLGA ratio of 1:4. After homogenization for 15 min at 25,000 rpm, the sample was magnetically stirred for 6 hr to allow acetone evaporation. To isolate the nanoparticles, the dispersion was ultracentrifuged at 25,000 rpm for 45 min at 4°C and settled pellets were redispersed in water. Subsequently, a freeze-drying process was employed to facilitate a better evaluation of the pellet. The samples were evaluated for responses by methods described in previous sections.

Characterization and evaluation of C-CFZ-PLGA-NPs

Scanning Electron Microscopy (SEM) and Transmission Electron Microscopy (TEM)

For SEM examination, the monolayer of C-CFZ-PLGA-NPs was affixed to a metallic substrate, followed by the application of a 10 nm-thick gold coating onto the particles using the gold sputtering method. Subsequently, the C-CFZ-PLGA-NPs were scrutinized using an SEM instrument (Zeiss, Germany) operating at 20 kV. The appearance of the C-CFZ-PLGA-NPs were evaluated using TEM (JEOL JEM 1010, Japan). On a copper grid, a single drop of CFZ-NPs dispersion made with Milli-Q water was applied, and it was left to dry. Before TEM investigation, the sample was air-dried to remove excess liquid and stained with phosphotungstic acid (1% w/w).

Fourier-Transform Infrared (FTIR) and Differential Scanning Calorimetry (DSC)

The spectra of pure CFZ, PLGA, PVA, chitosan, physical blend, and optimized C-CFZ-PLGA-NPs were obtained utilizing an FTIR spectrophotometer (Vertex 70v, Bruker, Bremen, Germany). A Perkin Elmer 4000 (MA, USA) calorimeter was used to examine the thermal characteristics of the CFZ, PLGA, PVA, Chitosan, Physical mixture, and C-CFZ-PLGA-NPs samples. The formulations were desiccator-dried for the duration of the night for this purpose. Then, powdered samples were put into lidded aluminum pans. After sealing, heating under nitrogen flow from 30 to 300°C (10°C per minute) was done.

In vitro CFZ release

C-CFZ-PLGA-NPs and CFZ dispersion were the subject of this testing utilizing the dialysis bag technique in a USP dissolving device (paddle type) with phosphate buffer (pH 7.4). Preactivated dialysis bags were filled with formulations containing 8 mg of drug in 2 mL, knotted at both ends, and submerged in the 900 mL medium at 37°C and 100 rpm for 48 hr. To maintain sink conditions, 5 mL aliquots were sampled and replaced with 5 mL of medium. After 48 hr, the percentage of CFZ release was estimated using UV-visible spectrophotometry on the collected samples, which was measured at 292 nm.

Cell viability study using MTT assay

HepG2 liver cancer cells were prepared for testing by seeding them (96-well; 5×10^3 cells/well) and letting them adhere overnight. The next day, they were exposed to different concentrations of nanoparticles (C-CFZ-PLGA-NPs and placebo NPs) and the drug CFZ for 24 hr (37°C). Cell viability was checked by MTT assay, where a formazan dye formation indicates live cells. The dye was dissolved and its absorbance measured (microplate reader),

providing data for analysis (Gen5™ software) and calculation of IC_{50} values (concentration inhibiting 50% of cell growth).

Storage stability testing

The optimized C-CFZ-PLGA-NPs were placed at 4°C for 90 days. These samples were evaluated at the intervals of 30 days for the assessment of PS, PDI, and ZP.

Statistics

Studies were performed in triplicate, and data were depicted as the Mean ± Standard Deviation (SD). The statistical significance was calculated using a one-way Analysis of Variance (ANOVA) with a Tukey multiple comparison test. The statistical differences were taken as significant at $p^* < 0.05$.

RESULTS

Preparation, optimization and evaluation of canagliflozin-loaded PLGA NPs

The PS, PDI, ZP, and EE of CFZ-loaded PLGA NPs were obtained for different CFZ: PLGA ratios and PVA levels and are provided in Table 1. The effects of the CFZ: PLGA ratio on the PS, PDI, ZP, and EE of the prepared CFZ-loaded PLGA NPs at a PVA level of 2.5, 5 and 7.5 mg/mL are shown in Table 1. The effect of PVA levels on various CFZ:PLGA ratios are shown in Figure 1(a-d).

From the results observed for the canagliflozin-loaded PLGA nanoparticles, the nanoparticles prepared with a CFZ: PLGA ratio of 1:4 and PVA level of 5 mg/mL were chosen for further studies (CFZ-PLGA-NPs). The PS, PDI, ZP, and EE for the selected NPs were 159 ± 1.0 nm, 0.149 ± 0.02 , -36.5 ± 3.52 mV, and $84.8 \pm 3.10\%$. The NPs with a CFZ: PLGA ratio of 1:1 and PVA level of 5 mg/mL had the lowest PS. However, the EE was very low with a value of $64.5 \pm 1.06\%$. Also, the PDI was higher than the selected formulation. Hence, this formulation was not considered. Meanwhile, the NPs with CFZ: PLGA ratio of 1:1 and PVA level of 2.5 mg/mL had a lower PS and PDI compared to the selected formulation. However, the EE was very less with $49.6 \pm 0.94\%$. Hence, this formulation was not considered.

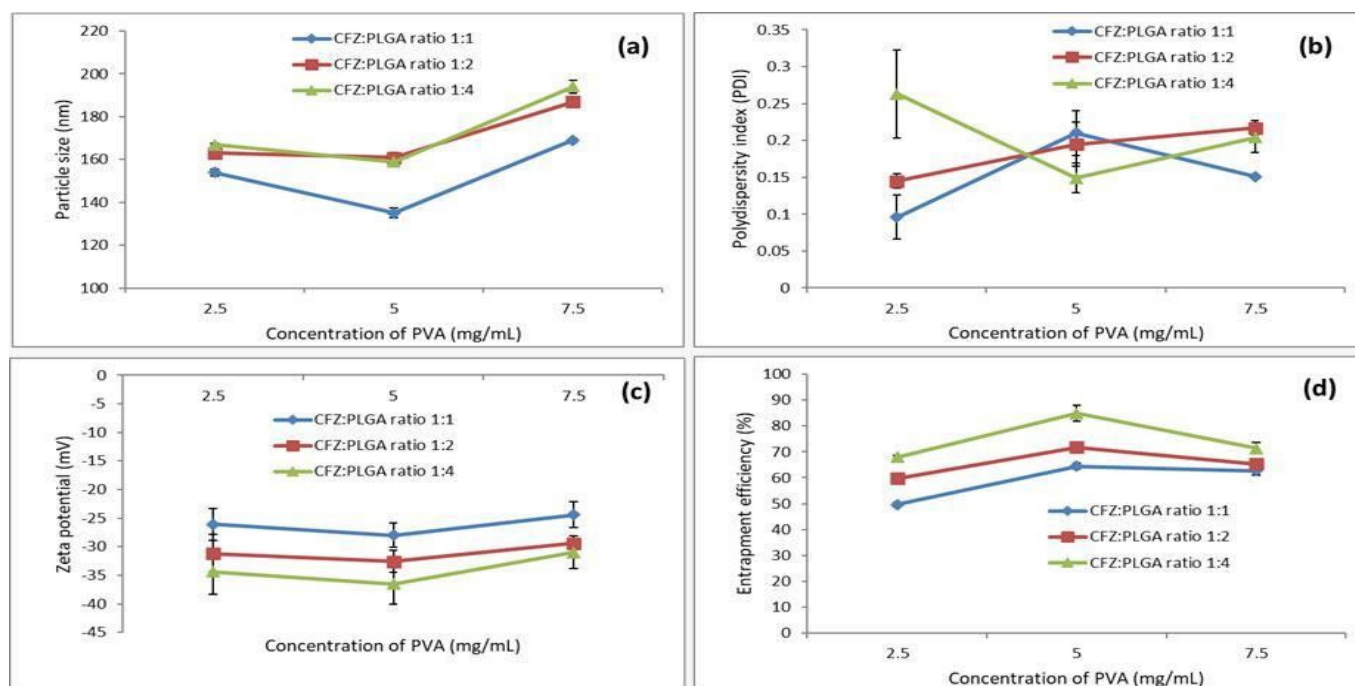
Formulation, optimization and evaluation of chitosan-coated PLGA NPs of canagliflozin

The chitosan-coated PLGA nanoparticles were prepared and evaluated with different chitosan concentrations, CFZ: PLGA ratio of 1:4 and PVA level of 5 mg/mL (Table 2). The PS, PDI, ZP, and EE of the prepared chitosan-coated PLGA nanoparticles of canagliflozin were determined.

The effects of chitosan concentration on the PS, PDI, ZP, and EE of the chitosan-coated PLGA NPs of CFZ are shown in Figure 2.

Table 1: Optimization of the CFZ: PLGA ratio and PVA level for the development of optimized nanoparticles of canagliflozin (\pm SD).

Drug: polymer ratio (CFZ: PLGA)	Stabilizer conc. (PVA; mg/mL)	PS (nm)	PDI	ZP (mV)	EE (%)
1:1	2.5	154 \pm 1.6	0.096 \pm 0.03	-26.1 \pm 2.83	49.6 \pm 0.94
1:2		163 \pm 1.6	0.145 \pm 0.01	-31.2 \pm 3.32	59.8 \pm 0.56
1:4		167 \pm 0.5	0.263 \pm 0.06	-34.4 \pm 3.97	68.0 \pm 0.60
1:1	5	135 \pm 2.3	0.210 \pm 0.03	-28.0 \pm 2.11	64.5 \pm 1.06
1:2		161 \pm 2.4	0.195 \pm 0.03	-32.6 \pm 1.91	71.8 \pm 0.79
1:4		159 \pm 1.0	0.149 \pm 0.02	-36.5 \pm 3.52	84.8 \pm 3.10
1:1	7.5	169 \pm 1.1	0.151 \pm 0.00	-24.4 \pm 2.31	62.7 \pm 1.62
1:2		187 \pm 1.0	0.217 \pm 0.01	-29.4 \pm 0.82	65.3 \pm 1.27
1:4		194 \pm 3.0	0.204 \pm 0.02	-31.0 \pm 2.88	71.4 \pm 2.16

**Figure 1:** Effect of PVA levels on (a) PS, (b) PDI, (c) ZP, and (d) EE at different CFZ:PLGA ratios.

Characterization and evaluation of chitosan-coated PLGA nanoparticles of canagliflozin (C-CFZ-PLGA-NPs).

Particle size distribution and Zeta Potential

Figure 3 (a-b) shows the representative PS distribution and ZP results obtained for the selected Chitosan-coated PLGA NPs of CFZ.

Scanning Electron Microscopy (SEM) and Transmission Electron Microscopy (TEM)

SEM and TEM images were observed for studying the surface morphology and actual particle size of the optimized C-CFZ-PLGA-NPs (Figure 3c-d).

Fourier-Transform Infrared (FTIR) and Differential Scanning Calorimetry (DSC) analysis

The FTIR spectra and DSC thermograms of the samples are shown in Figure 4a-b.

In vitro CFZ release

The release of CFZ from C-CFZ-PLGA-NPs was compared with the release from its aqueous dispersion by the dialysis bag method. From C-CFZ-PLGA-NPs, the CFZ release was notably higher at all sampling points (Figure 5a). After 48 h of study, 80.9 \pm 1.2% release of CFZ was noted from C-CFZ-PLGA-NPs whereas only a 25.9 \pm 1.4% release was observed from CFZ dispersion.

Cell viability by MTT assay

The cell viability studies carried out in HepG2 cells for C-CFZ-PLGA-NPs and pure CFZ as shown in Figure 5b). The cell viability shown by the placebo NPs was notably higher ($p < 0.01$) than those produced by C-CFZ-PLGA-NPs and pure CFZ. The placebo NPs were considered non-cytotoxic up to concentrations of 25 $\mu\text{g/mL}$ and weakly cytotoxic for concentrations of 50 and 100 $\mu\text{g/mL}$. At studied concentrations of 3.125 and 6.25 $\mu\text{g/mL}$, there were no statistically significant variations ($p > 0.05$) between the cell viability produced by C-CFZ-PLGA-NPs and CFZ samples. The IC_{50} were 26.24 ± 1.43 and 12.54 ± 0.66 $\mu\text{g/mL}$ for pure CFZ and C-CFZ-PLGA-NPs respectively.

Storage stability testing

The results of storage stability testing are provided in Figure 5C-E. There were no significant variations between the PS of stored C-CFZ-PLGA-NP samples. The particle size was found to be stable over the entire testing period of 90 days.

DISCUSSION

Preparation, optimization and evaluation of canagliflozin-loaded PLGA NPs

All the trials resulted in CFZ-loaded PLGA NPs with a PS below 200 nm. The use of acetone as the organic phase for dissolving PLGA and CFZ might have significantly contributed to such lower particle sizes.^{17,18}

The effects of the CFZ:PLGA ratio on the PS, PDI, ZP, and EE of the prepared CFZ-loaded PLGA NPs at a PVA level of 2.5 mg/mL. The PS showed an increase when the CFZ: PLGA ratio was increased. The CFZ: PLGA ratio of 1:4 resulted in significantly higher ($p < 0.05$) PS compared to those produced by CFZ: PLGA ratios of 1:1 and 1:2. Moreover, there was significant ($p < 0.05$) difference between PS produced by CFZ: PLGA ratios of 1:1 and 1:2. The first stage of the process of nanoprecipitation of PLGA in the present study involved the formation of droplets of acetone containing CFZ and PLGA, Later the acetone with high affinity for the aqueous phase diffuses into the bulk leaving

Table 2: Optimization of chitosan coating CFZ-PLGA-NPs.

Chitosan concentration (%)	Drug: polymer ratio (CFZ: PLGA)	PVA level (mg/mL)	PS \pm SD (nm)	PDI \pm SD	ZP \pm SD (mV)	EE \pm SD (%)
0.25	1:4	5	277 \pm 23	0.241 \pm 0.011	57.2 \pm 0.67	80.5 \pm 1.78
0.50			409 \pm 9.0	0.271 \pm 0.009	63.6 \pm 1.40	74.2 \pm 1.41
0.75			1224 \pm 67	0.585 \pm 0.048	65.4 \pm 0.76	58.6 \pm 1.50

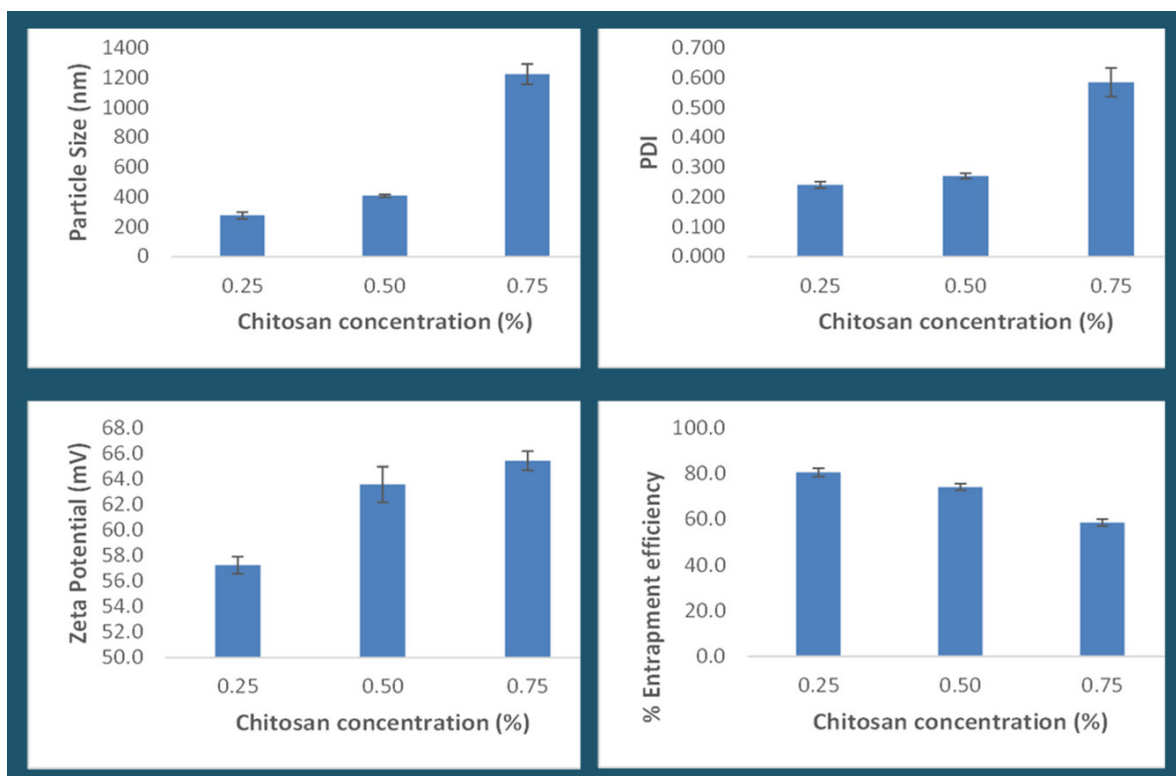
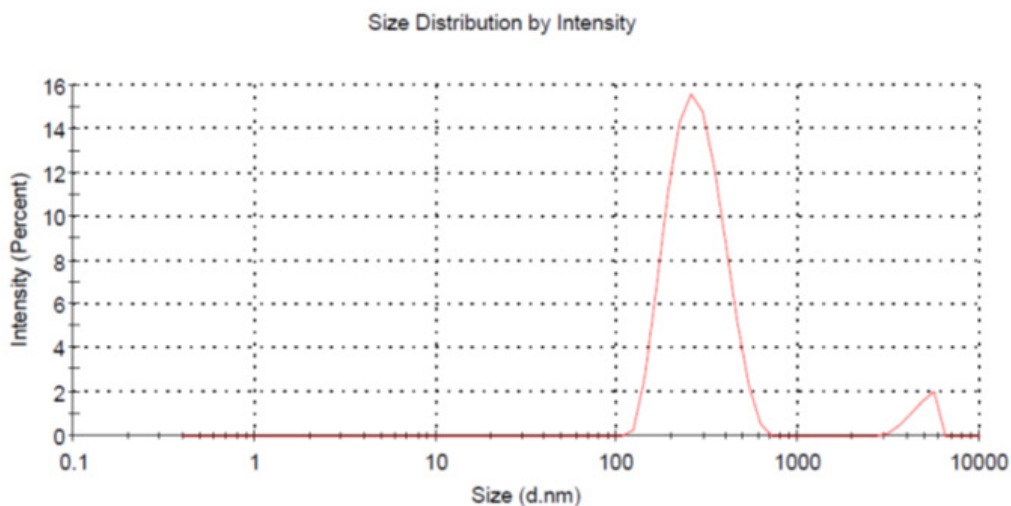


Figure 2: Effect of chitosan concentration on PS, PDI, ZP, and EE.

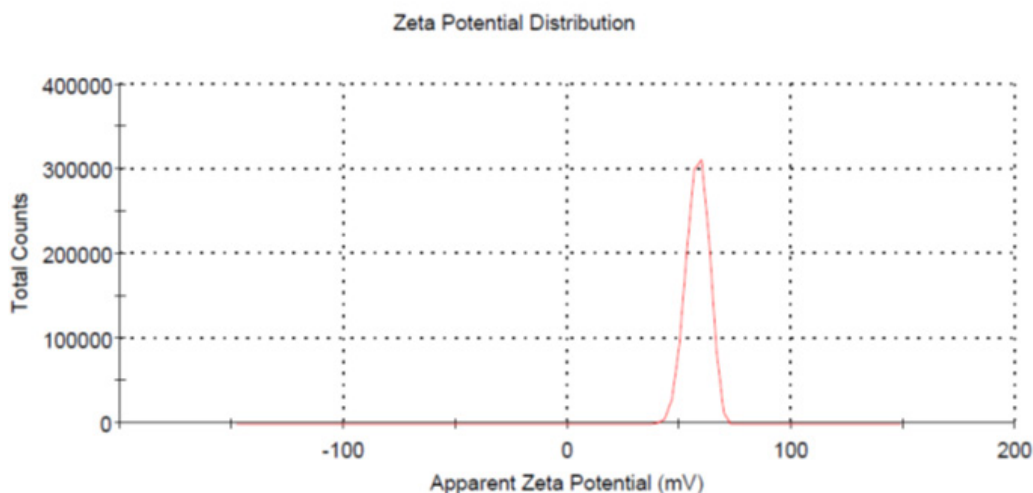
behind the CFZ-loaded PLGA NPs. Thus, nanoprecipitation by solvent diffusion has been better than the solvent evaporation method in the case of PLGA nanoparticles.¹⁹ Meanwhile, when the amount of PLGA increases, the resultant CFZ-loaded PLGA NPs will be having increased PS, owing to higher PLGA content in each drop of the acetone. Thus, the present observation of an increase in PS with an increase in PLGA in the acetone is well reasonable. Furthermore, similar results with a linear increase in PS of PLGA NPs with an increase in polymer concentration were demonstrated with PLGA nanoparticles.²⁰ Now considering the effect of the CFZ: PLGA ratio on PDI, the observed results were similar to that observed for PS. Notably, while the effect of the drug: polymer ratio is studied and described in most of the studies on PLGA NPs by nanoprecipitation, the effect on PDI remains ignored or unexplained. Therefore, we present an explanation based on the acetone migration effect to the aqueous phase as a possible reason for the observed results of PDI. This

proposal is inspired from a reported alcohol migration effect in nanoemulsion.²¹ We propose that at higher PLGA concentrations, the diffusion of acetone might be more erratic owing to the presence of a high concentration of PLGA in each acetone globule. Thus, the amount of acetone diffusion into the aqueous phase may be slightly different from each globule. These effects result in NPs with slightly different PS and subsequently NPs with higher polydispersity. Finally, the measured PDI would be more for trials with higher PLGA content. Thus, the PDI value of NPs prepared with CFZ: PLGA ratio of 1:4 was significantly higher ($p < 0.05$) compared to those produced by CFZ: PLGA ratios of 1:1 and 1:2.

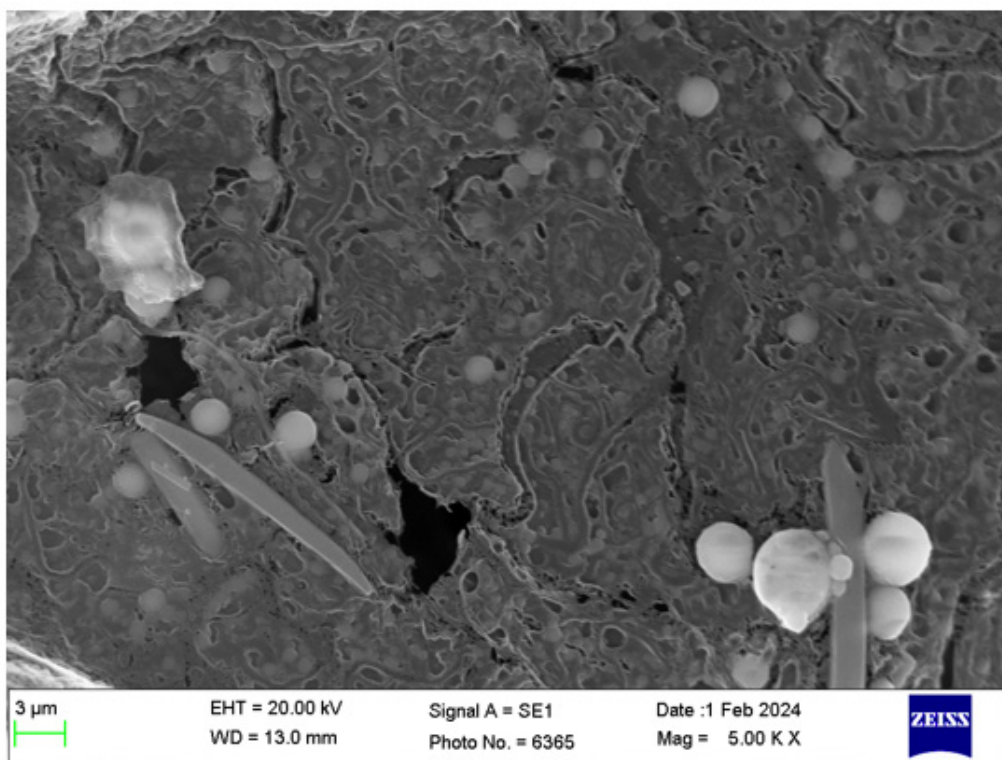
The ZP values were with negative signs and the magnitudes were greater than 25 mV for all the NPs. PLGA is a polymer of d, l-lactic-co-glycolic acid and it is reasonable that nanoparticles formed with this polymer show negative surface



A)



b)



C)

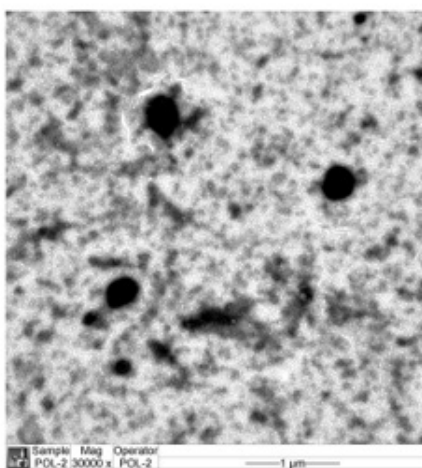


Figure 3d

D)

Figure 3: Particle size distribution (A) and zeta potential (B) Scanning electron microscopy (c) and transmission electron microscopy (d) images of C-CFZ-PLGA-NPs.

charge. Furthermore, the negative change of PLGA NPs is well established.²² The magnitude of ZP of the PLGA NPs increased with an increase in the amount of PLGA (or a decrease in CFZ: PLGA ratio). This effect can be explained by the fact that NPs formed at higher amounts of PLGA have increased charge for each particle due to higher PLGA content. Thus, the charge on the PLGA NPs prepared with a CFZ: PLGA ratio of 1:4 was the

highest observed ZP. However, there was no significant ($p > 0.05$) variation between the ZP values of the PLGA NPs. The EE was another response chosen for the evaluation of the effect of the CFZ: PLGA ratio. There was a highly significant variation ($p < 0.001$) between the EE observed for the studied CFZ: PLGA ratio of 1:1, 1:2, and 1:4. The explanation of enhanced EE on increasing the amount of PLGA is obvious from the fact that

a higher amount of PLGA retains or entraps higher amount of CFZ in the nanoparticles during the diffusion of acetone into the aqueous phase. Furthermore, the hydrophobic nature of both CFZ and PLGA might have contributed to the higher retention of CFZ in the PLGA matrix of NPs and subsequently resulted in higher EE.

The effects of the CFZ:PLGA ratio on the PS, PDI, ZP, and EE of the prepared CFZ-loaded PLGA NPs at a PVA level of 5 mg/mL. A highly meaningful increase ($p < 0.001$) in PS was observed when the CFZ: PLGA ratio was changed from 1:1 to 1:2. However, there was no significant variation between PSs observed for CFZ: PLGA ratios of 1:2 to 1:4. In contrast to the PS of PLGA NPs produced with PVA level of 2.5 mg/mL, a decrease in PS was shown by changing the CFZ: PLGA ratio from 1:2 to 1:4. The ability of residual PVA to decrease the PS has been previously established.²³ This might have contributed to the observation of PS with a PVA level of 5 mg/mL. In addition to PS, the trend of PDI with respect to CFZ: PLGA ratio was considerably different for 2.5 and 5 mg/mL of PVA level. The mean PDI values decreased with increasing PLGA amount for 5 mg/mL of PVA level. The effect of a decrease in PDI by increasing PVA level has been demonstrated.²⁴ Thus, a decrease in PDI at higher PVA level in the present study could be justified. However, it is noteworthy that there was no significant variation between the PDI values observed for CFZ:PLGA ratios of 1:1, 1:2, and 1:4 for 5 mg/mL of PVA level. This indicated that a PVA level of 5 mg/mL could be sufficient or optimum to produce PLGA NPs of low and stable PDI values.

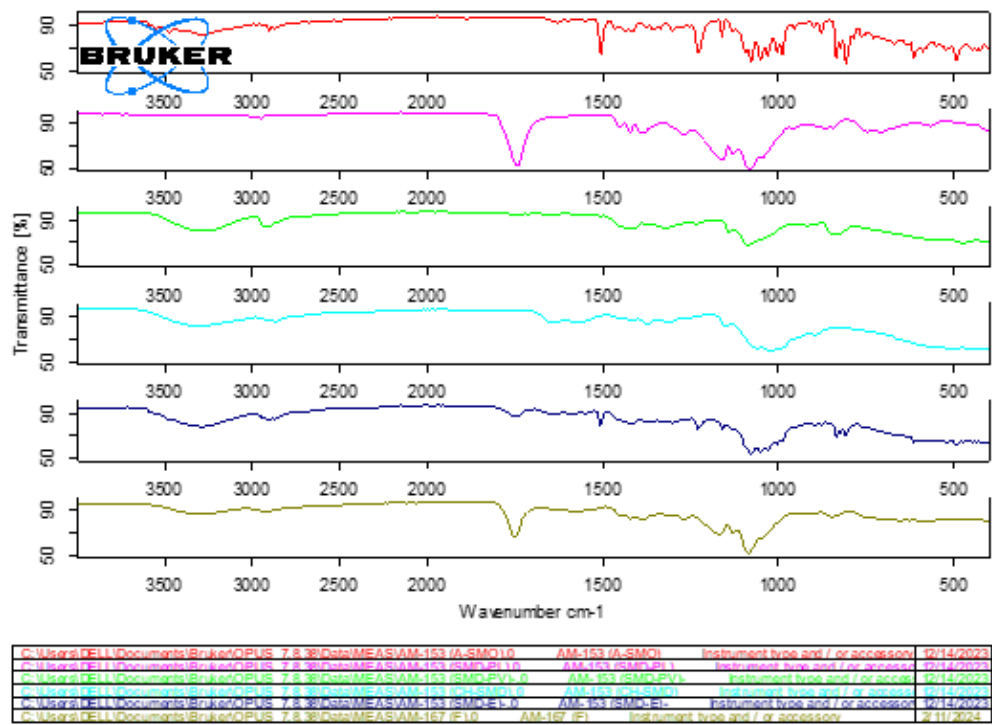
At a PVA level of 5 mg/mL, the ZP values showed a gradual increase in the mean value on changing the CFZ: PLGA ratio from 1:1 to 1:4. However, there was no statistically meaningful variation ($p > 0.05$) between the observed ZP values. It was previously demonstrated that higher PVA reduces the zeta potential of PLGA NPs.²⁵ However, it was observed for the microfluidics method and cannot be directly correlated to the conditions of our present study.²⁶ Nevertheless, the absence of any statistically meaningful variation in ZP might be due to the influence of such an effect in the present study. Moreover, interestingly, an increase in the magnitude of zeta potential with negative charge was observed on increasing PVA level.²⁷ The adsorption of PVA on NPs was suggested to cause such an effect. A similar situation exists in the present study too, where the PVA stabilizer can adsorb over the formed PLGA NPs. Meanwhile, the EE of the PLGA NPs was found to be significantly influenced by both the CFZ:PLGA ratio and concentration of PVA. The EE increased considerably ($p < 0.01$) when the CFZ: PLGA ratio was changed from 1:1 to 1:4. As observed and discussed in the previous section, a higher amount of PLGA in the acetone droplets could enhance the entrapment of CFZ in the PLGA NPs and thus can result in higher EE values. Coming to the role of PVA in the EE, a significant variation ($p < 0.05$) was observed for PVA levels of 2.5 and 5 mg/mL. The EE values were considerably higher for a

PVA level of 5 mg/mL. In general, higher concentrations of PVA stabilizer could decrease the EE of PLGA NPs.^{28,29} However, from the observed results, it could be reasonably assumed that the effect of the higher amount of PLGA could have outperformed the effect of PVA resulting in higher EE values.

The effects of the CFZ:PLGA ratio on the PS, PDI, ZP, and EE of the prepared CFZ-loaded PLGA NPs at a PVA level of 7.5 mg/mL. The mean PS increased with an increase in the amount of PLGA. Furthermore, there was a considerable ($p < 0.05$) variation between the observed PS for different CFZ:PLGA ratios. This increase in PS might be attributed to the higher PLGA amount used as discussed in previous sections and was in accordance with reported results.²⁸ Meanwhile, compared to the effect of PVA level of 2.5 and 5 mg/mL on PS, 7.5 mg/mL had appreciably ($p < 0.05$) higher PS at the corresponding CFZ: PLGA ratio. Such an effect of enhancement of PS by increased PVA level was established in earlier studies²⁸. However, a decrease in PS by PVA was also established.²³ Nevertheless, from the results of the present study, we could assume that the PVA level of 7.5% was insufficient to overcome the effects of PLGA amount at CFZ:PLGA ratios of 1:1 to 1:4 on increasing the mean PS of PLGA NPs. Furthermore, a reported study demonstrated an initial decrease in PS and later an increase in PS of PLGA NPs on changing PVA level from 1 to 5%.³⁰ Thus, it could be concluded that a PVA level of 7.5 mg/mL supports the increase in the PS of PLGA NPs.

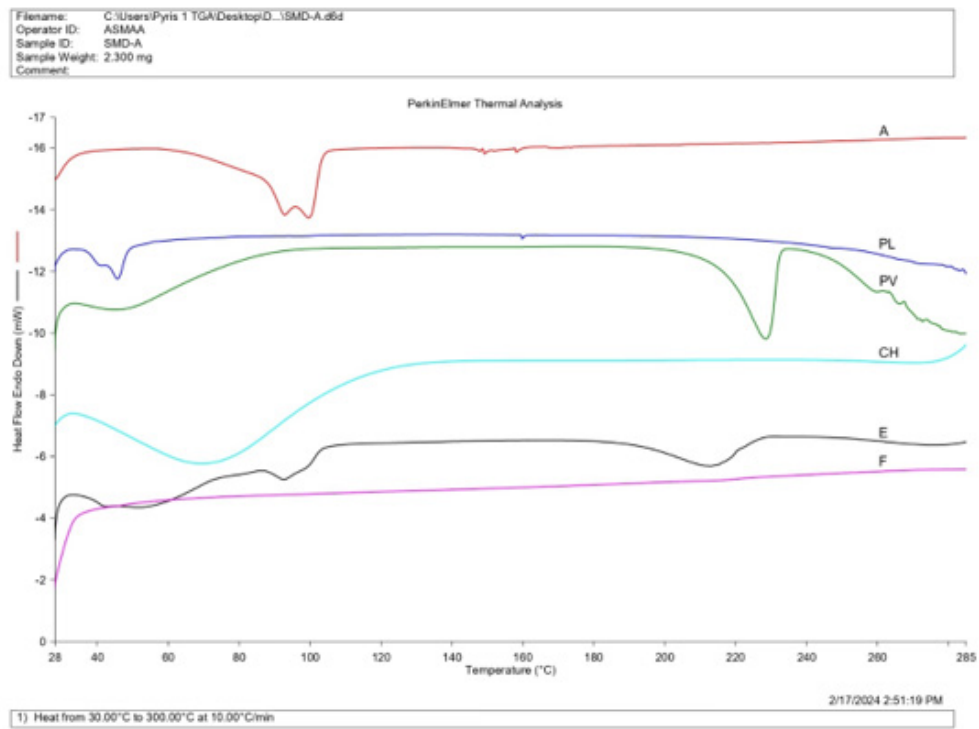
A conclusion about the effect of PVA levels on various CFZ:PLGA ratios can be derived from Figure 1a. At all studied CFZ: PLGA ratios, the PS decreased when the PVA level increased from 2.5 to 5 mg/mL, and later the PS increased when the PVA level was further increased to 7.5 mg/mL. In addition, the CFZ:PLGA ratio provided the lowest PS values for all the PVA levels studied. A further increase in the CFZ:PLGA ratio did not produce a noteworthy effect on PS for a specific PVA level.

Meanwhile, the PDI did not show a pattern or trend with respect to CFZ: PLGA at a PVA level of 7.5 mg/mL. However, the PDI at a CFZ:PLGA ratio of 1:1 was considerably ($p < 0.01$) lower than those produced by ratios of 1:2 and 1:4. As discussed earlier, higher PLGA amount can possibly enhance the PDI by interfering with the diffusion of acetone in the nanoprecipitation method and finally resulting in higher polydispersity. Now considering the effect of PVA level on PDI, it can be seen that (Figure 1b) the effect is dependent on the CFZ:PLGA ratio. For the CFZ:PLGA ratio of 1:1, the PDI first increases and later decreases on increasing the PVA level from 5 to 7.5 mg/mL. The CFZ:PLGA ratio of 1:2 produces a linear increase in PDI with increasing the PVA level. In the case of CFZ:PLGA ratio of 1:4, the PDI first decreases upon changing the PVA level from 2.5 to 5 mg/mL, and a further increase in PVA level to 7.5 mg/mL increases the PDI. Thus, it could be derived that the PDI could be tailored by selecting the appropriate CFZ:PLGA ratio for the preparation of PLGA NPs.



Page 1/1

a)



b)

Figure 4: (A) FTIR spectra and (B) DSC thermogram of different samples. (a) CFZ raw powder, (PL) PLGA, (PV) PVA, (CH) Chitosan, (E) physical mixture, and (F) C-CFZ-PLGA-NPs.

The ZP values showed a gradual increase in the mean value on changing the CFZ: PLGA ratio from 1:1 to 1:4. However, there was considerable variation ($p < 0.05$) in ZP among CFZ:PLGA ratios of 1:1 and 1:4 only. As suggested earlier, the adsorption of the PVA stabilizer on the PLGA NPs could have contributed to a higher magnitude of ZP at higher CFZ:PLGA ratios. The overall effect of the studied PVA levels on ZP is provided in Figure 1c. A clear enhancement of the magnitude of ZP was observed on changing the CFZ:PLGA ratio from 1:1 to 1:4. In the case of CFZ:PLGA ratios of 1:1 to 1:2, there was no noteworthy effect of PVA level on ZP. However, at a CFZ:PLGA ratio of 1:4, the ZP first increased in magnitude when the PVA level was increased from 2.5 to 5 mg/mL and further increasing of PVA level to 7.5 mg/mL decreased the magnitude of ZP.

The EE of the PLGA NPs with a PVA level of 7.5 mg/mL showed a similar pattern observed for 2.5 and 5 mg/mL concentrations. The EE was appreciably higher ($p < 0.05$) for the CFZ:PLGA ratio of 1:4 compared to that of others. However, no considerable variation ($p > 0.05$) was observed between the effects of CFZ:PLGA ratios 1:1 and 1:4. As explained earlier, the effect of PLGA on enhancing the EE must have outperformed any effect of PVA on EE. The combined effect of PVA level on EE was determined from Figure 1d. For all the studied CFZ:PLGA ratios, EE increased when the PVA level increased from 2.5 to 5 mg/mL. Further increase of PVA level to 5 mg/mL resulted in a decrease in the EE. In the case of the CFZ:PLGA ratio of 1:1, this final decrease in EE was insignificant. A similar change in the pattern of EE on changing the PVA level was noted in a previous study.³⁰

Further PS in the range of 50-200 nm and PDI below 0.3 are considered suitable for *in vivo* use.^{18,31} The selected formulation had low PS and low PDI. Furthermore, this formulation had the highest magnitude for zeta potential and entrapment efficiency compared to all other canagliflozin-loaded PLGA nanoparticles. Therefore, the selected formulation was considered most suitable for further studies. The PS, PDI, ZP, and EE for the selected NPs were 159 ± 1.0 nm, 0.149 ± 0.02 , -36.5 ± 3.52 mV, and $84.8 \pm 3.10\%$.

Formulation, evaluation, and optimization of chitosan-coated PLGA NPs of canagliflozin

The effects of chitosan concentration on the PS, PDI, ZP, and EE of the chitosan-coated PLGA NPs of CFZ are shown in Figure 2. The PS was found to increase linearly with an increase in the chitosan concentration. There was a considerable variation ($p < 0.05$) between the PS of NPs prepared with 0.25 and 0.5% chitosan. Meanwhile, the PS of NPs prepared with 0.75% chitosan had an extensive variation ($p < 0.001$) with the other two chitosan concentrations. Such an effect of enhancement of PS of PLGA NPs on chitosan coating was previously demonstrated.²² Furthermore, the increase in PS of chitosan-coated PLGA NPs with an increase in chitosan concentration is also reported.⁴ The positive charge on chitosan molecules, surface free energy,

and surface non-uniformity-dependent mechanisms were suggested for the concentration-dependent chitosan adsorption onto PLGA NPs.³² Meanwhile, the PDI also followed a similar pattern shown by the PS. The PDI values increased by increasing the chitosan concentration. The PDI was found to be unaffected by chitosan coating in a reported study even when an increase in PS was observed.²² However, in that reported study chitosan concentration of 0.1% was used and was much lesser than the concentrations used in the present study. Therefore, such an effect cannot be expected in the present study. There was no major variation ($p > 0.05$) between the PDI values observed for 0.25 and 0.5% chitosan concentrations. The PDI value was much higher ($p < 0.001$) for chitosan concentration of 0.75% compared to other studied concentrations. The increased viscosity of chitosan solution and uncontrollable surface adsorption of chitosan onto PLGA nanoparticles could be the possible reasons for the formation of polydisperse NPs and subsequently high PDI values at chitosan concentration of 0.75%.

The chitosan coating was well established by the change in the sign of ZP values. The sign was positive for all the chitosan-coated NPs whereas the uncoated PLGA NPs described in the previous sections had a negative sign for ZP. This result was in good agreement with reported studies.^{4,22} Furthermore, it is obvious that the negative charge of PLGA molecules favors adsorption and subsequent coating of chitosan over the NPs. The ZP was significantly lesser ($p < 0.001$) at 0.25% compared to 0.5 and 0.75% chitosan. However, there was no major variation ($p > 0.05$) between the ZP values produced by 0.5 and 0.75% chitosan. Furthermore, it was noteworthy that the ZP values were very high and above 57 mV for all the chitosan-coated NPs. This has tremendous implications for high stability and enhanced cancer cell death rendering it a highly attractive platform for tumor-targeted drug delivery.³³ However, such an increase in the ZP value was associated with a lowering of entrapment efficiency in the present study. Nevertheless, such a decrease in EE was not much affected at a chitosan concentration of 0.25%. It still retained an EE of $80.5 \pm 1.78\%$ and was much comparable to the EE of uncoated PLGA NPs ($84.8 \pm 3.10\%$). The EE decreased drastically to $58.6 \pm 1.50\%$ when the chitosan concentration was 0.75%. It was noted that the EE at all the chitosan concentrations was considerably dissimilar ($p < 0.01$). Interestingly, the loss of surface adsorbed drug during the repeated centrifugation steps in chitosan-coated NPs has been suggested for such a decrease of EE.⁴

Based on the results of the evaluation of chitosan-coated PLGA NPs of CFZ, formulation prepared with 0.25% chitosan, CFZ: PLGA ratio of 1:4, and PVA level of 5 mg/mL was chosen for further characterization and evaluation (C-CFZ-PLGA-NPs). The selection was based on the lowest PS, lowest PDI, and highest EE. Even though the ZP was lowest for this formulation compared to those prepared with other chitosan concentrations,

the observed value of 57.2 ± 0.67 mV was extremely high and therefore acceptable.

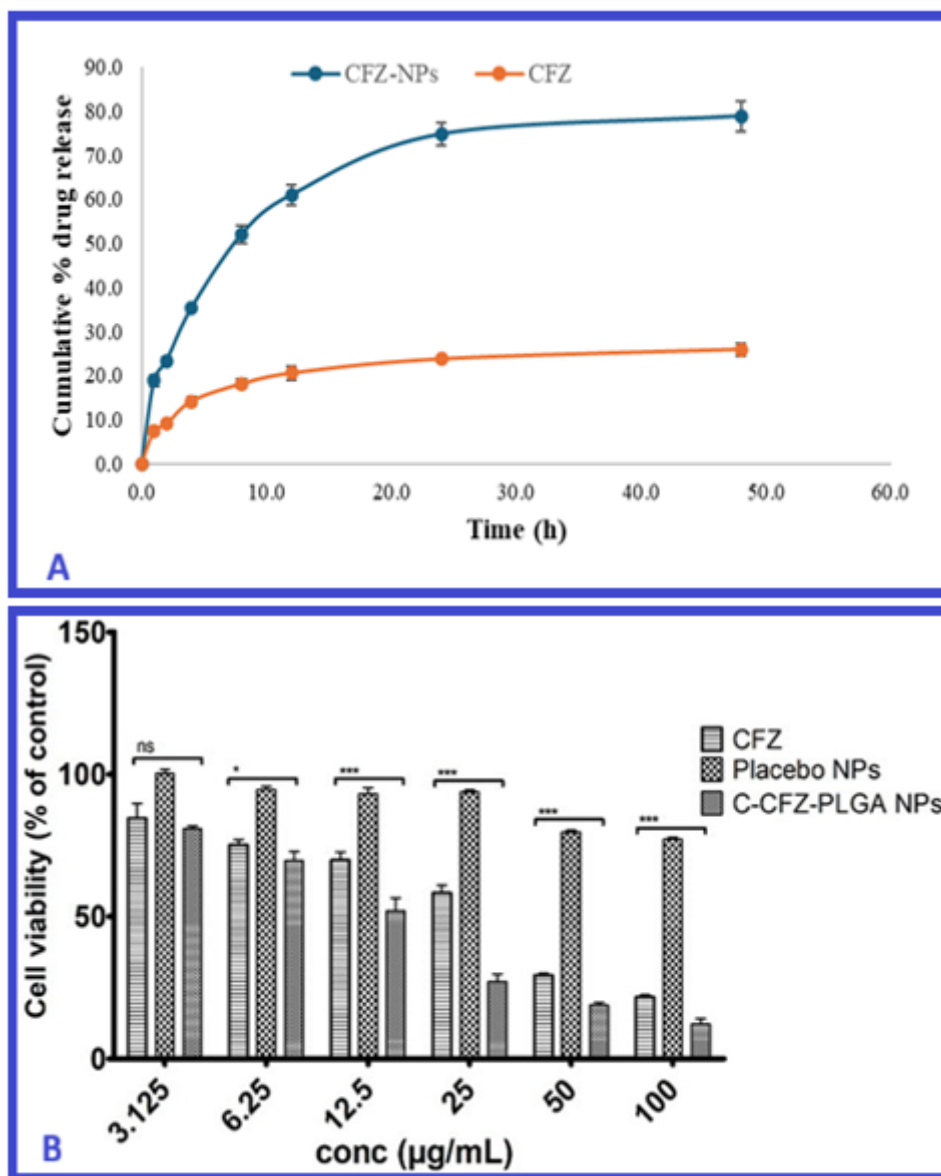
Characterization and evaluation of chitosan-coated PLGA nanoparticles of canagliflozin (C-CFZ-PLGA-NPs)

The SEM images confirmed the spherical structure and less smooth surface morphology of the C-CFZ-PLGA-NPs. It has been reported that PLGA nanoparticles have a very smooth surface compared to chitosan-coated surfaces when examined for the SEM image.³⁴ A very similar SEM image was observed for the optimized C-CFZ-PLGA-NPs.

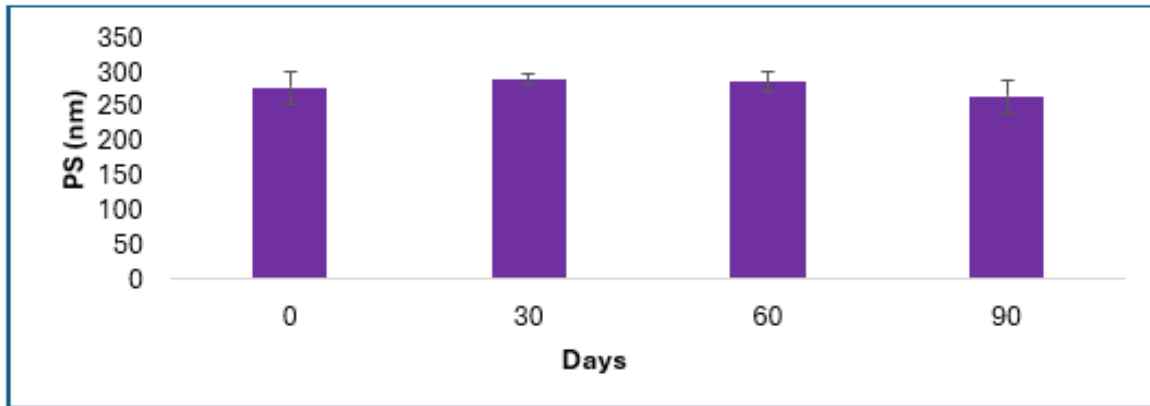
The hydrodynamic PS obtained from Zetasizer showed similar results as observed in TEM images. TEM image of the C-CFZ-PLGA-NPs showed a spherical morphology with a solid

dense PLGA core and even distribution of chitosan coating and was comparable to a reported observation of chitosan-coated PLGA NPs.³⁵ The interactions of positively charged chitosan and negatively charged PLGA NPs can be considered responsible for such an observation.³⁴

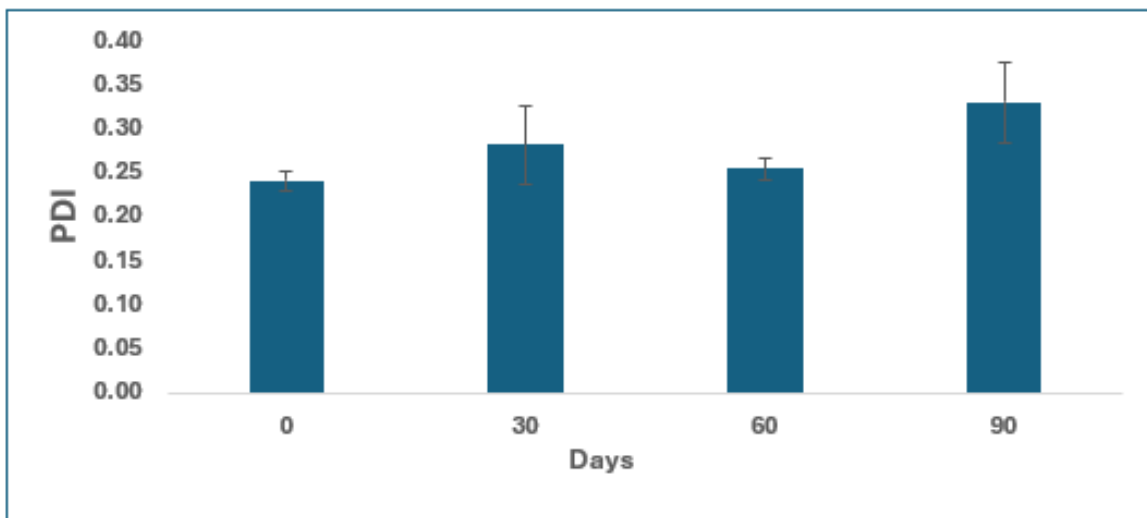
The FTIR spectrum of CFZ complied with reported peaks at around 3480 (OH stretch), 3287 (aromatic C-H stretch), 1445 (aromatic C=C stretch), 2900 (C-H stretch of CH_3), and 1229 cm^{-1} (Aryl C-F stretch).³⁶ Similarly, the FTIR spectrum of PLGA strongly complied with the reported peaks at around 1094 (C-O-C stretch) and 1758 cm^{-1} (C=O stretch).³⁴ Meanwhile, the characteristic peaks of PVA were identified in its FTIR spectrum. Characteristic peaks were found at around 3250 (O-H stretch) and 2936 cm^{-1} (asymmetric stretch of CH_2).^{37,38} Chitosan showed



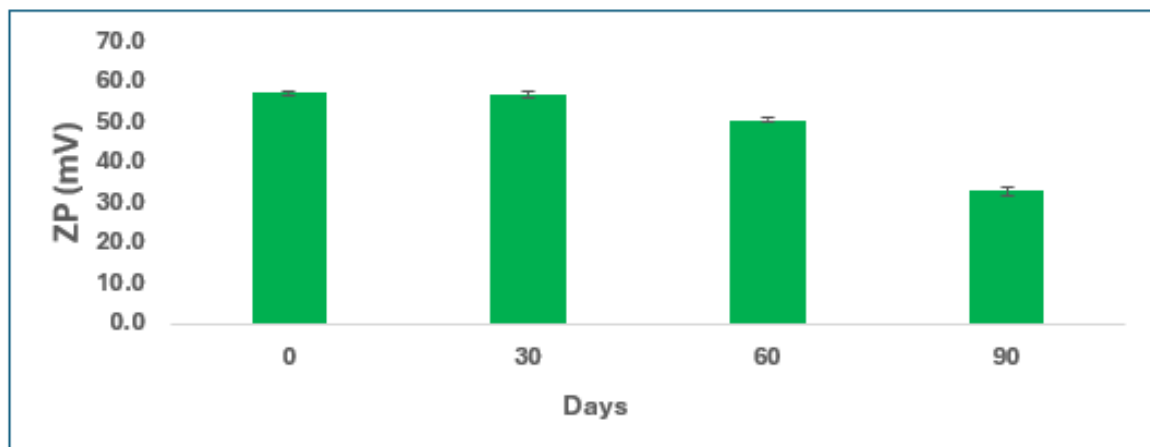
A) and B)



(C)



(D)



(E)

Figure 5: (A) *In vitro* CFZ release profiles of CFZ dispersion and C-CFZ-PLGA-NPs at pH 7.4 by dialysis method. (B) Cell viabilities of HepG2 cells by MTT assay after treatment with Canagliflozin (CFZ), Placebo nanoparticles (Placebo NPs), and C-CFZ-PLGA-NPs. (C) Particle Size (PS), (D) PDI, and (E) Zeta Potential (ZP) values of C-CFZ-PLGA-NPs at 4°C during the storage stability experiment.

its typical FTIR spectrum reported in the literature with peaks at around 3440 (NH₂ and OH stretch), 1650 (amide C=O), and 1100 cm⁻¹(C-O stretch).³⁹ The FTIR spectrum of the physical mixture showed an effect of lowering the peak intensities owing to the dilution of the samples. It was interesting to note that the FTIR spectrum of C-CFZ-PLGA-NPs was predominantly similar to that of PLGA owing to the high content of PLGA in it. Also, the characteristic peak of chitosan at around 3440 cm⁻¹ was observed. Such a strong resemblance of FTIR spectra of PLGA and chitosan-coated PLGA NPs was observed in a previous study also.²²

The thermogram of CFZ showed its typical peak at around 100°C.⁴⁰ Meanwhile, the thermogram of PLGA showed typical endothermic peaks at around 45.62°C (glass transition) and was well relatable to reported thermograms.^{41,42} PVA also showed established and reported peaks at around 228 (melting) and 40-42.5°C (glass transition).⁴³ Chitosan exhibited its characteristic broad peak around 72.10°C owing to the vaporization of any residual solvents in it.⁴⁴ The physical mixture displayed the characteristic peak of CFZ and PLGA but with reduced intensity due to the possible dilution effect in the sample. Meanwhile, the sharp peaks of the individual samples disappeared in the C-CFZ-PLGA-NPs indicative of the conversion of the crystalline nature of CFZ and excipients to an amorphous one.⁴⁵

The *in vitro* release profile demonstrated that C-CFZ-PLGA-NPs appreciably enhance the CFZ release compared to its aqueous dispersion. The enhancement of apparent solubility of CFZ in the chitosan-coated PLGA NPs could be considered responsible for the observed results.⁴⁶

Cell viability by MTT assay

The cell viability studies carried out in HepG2 cells showed a major enhancement of cytotoxicity of C-CFZ-PLGA-NPs compared to pure CFZ. The placebo NPs were considered non-cytotoxic up to concentrations of 25 µg/mL.⁴⁷ The effect of osmotic pressure might have caused some minor cytotoxic effects at higher concentrations.⁴⁸ The results of IC₅₀ also indicated the enhancement of cytotoxicity of C-CFZ-PLGA-NPs as compared to CFZ. A similar enhancement of the cytotoxic effect of CFZ by formulation of NPs was observed in a previous study also.⁴⁹

Stability study

Some reported studies observed a slight increase in PS in the storage of chitosan-coated PLGA NPs.^{35,50} However, such an observation was not made in the stored C-CFZ-PLGA-NP samples. This indicated the absence of any significant chitosan swelling in the stored C-CFZ-PLGA-NPs. However, slight and irregular changes in PDI values were observed in the stored C-CFZ-PLGA-NP samples. Interestingly, both unchanged PDI and increased PDI have been observed after the storage of chitosan-coated PLGA NPs.^{35,50} Therefore, further studies may

be needed to explore the exact mechanism for the observations. Meanwhile, a notable decrease in the ZP was observed for the stored C-CFZ-PLGA-NPs after 30 days. Such a reduction in the magnitude of ZP of chitosan-coated PLGA NPs has already been reported.⁵⁰ However, the ZP of the stored C-CFZ-PLGA-NPs was around 33 mV even after 90 days. Nanoparticles with ZP values higher than ±30 mV are kinetically stable.⁵¹ Therefore, the C-CFZ-PLGA-NPs were considered to have sufficient storage stability in terms of ZP.

CONCLUSION

The present study evaluated the effects of different CFZ: PLGA ratios and PVA levels on PS, PDI, ZP, and EE of CFZ-loaded PLGA NPs when prepared by the nanoprecipitation method. Both the CFZ:PLGA ratio and PVA level were found to affect one or more responses. The formulation with CFZ:PLGA ratio of 1:4 and PVA level of 5 mg/mL, with PS of 159±1.0 nm, PDI of 0.149±0.02, ZP of 36.5±3.52 mV, and EE of 84.8±3.10%, was selected as the optimized one (CFZ-PLGA-NPs). A chitosan concentration of 0.25% was found to be optimum for the formulation of C-CFZ-PLGA-NPs. They had PS of 277±23 nm, PDI of 0.241±0.011, ZP of 57.2±0.67 mV, and EE of 80.5±1.78%. The SEM and TEM images confirmed the spherical nature and presence of chitosan coating on the C-CFZ-PLGA-NPs. Meanwhile, the FTIR, and DSC analysis confirmed the identity of individual components and the amorphous nature of the drug in the C-CFZ-PLGA-NPs. The notably higher CFZ release in pH 7.4 from C-CFZ-PLGA-NPs compared to a CFZ dispersion confirmed these results. The MTT assay in HepG2 cells demonstrated significant enhancement of cytotoxicity by C-CFZ-PLGA-NPs. The storage stability studies conducted at 4°C for 90 days confirmed the physical stability of C-CFZ-PLGA-NPs in terms of PS, PDI, and ZP. Thus, the present study demonstrated stable and effective C-CFZ-PLGA-NPs against hepatic cancer cells which could be further studied for preclinical and clinical efficacy.

ACKNOWLEDGEMENT

This project was funded by the Deanship of Scientific Research (DSR) at King Abdulaziz University, Jeddah, Saudi Arabia under grant no. (G:127-166-1442). The authors therefore acknowledge with thanks DSR for technical and financial support.

ABBREVIATIONS

CFZ: Canagliflozin; **PLGA:** Poly(lactic-co-glycolic acid); **NPs:** Nanoparticles; **C-CFZ-PLGA-NPs:** Chitosan coated poly(lactic-co-glycolic acid) nanoparticles; **PVA:** Polyvinyl Alcohol; **DSC:** Differential scanning calorimetry; **FTIR:** Fourier Transform Infrared Spectroscopy; **PS:** Particle size; **PDI:** Polydispersity index, **EE:** Entrapment efficiency; **ANOVA:** Analysis of variance; **nm:** Nanometer; **TEM:** Transmission electron microscopy; **ZPs:** Zeta Potential; **SEM:** Scanning electron

microscopy; **DSC**: Differential scanning calorimetry; **MTT**: 3-(4,5-di methyl thiazol-2-yl)-2,5-diphenyltetrazolium bromide; **SGLT2**: Sodium-glucose co-transporter-2; **HepG2**: Human liver cancer cells.

FUNDING

This project was funded by the Deanship of Scientific Research (DSR) at King Abdulaziz University, Jeddah, Saudi Arabia under grant no. (G:127-166-1442).

CONFLICT OF INTEREST

The authors declare that there is no conflict of interest.

SUMMARY

Canagliflozin (CFZ), an approved antidiabetic agent, has reported activities against the proliferation of liver cancer cells. Given the established biocompatibility, biodegradability, and the success of chitosan-coated Poly (Lactic-Co-Glycolic Acid) (PLGA) Nanoparticles (NPs) in delivering drugs to cancer cells, this study focused on developing nanoparticles specifically loaded with CFZ (C-CFZ-PLGA-NPs). Firstly, optimization of the formulation of CFZ-loaded PLGA NPs (CFZ-PLGA-NPs) by nanoprecipitation was carried out. Polyvinyl alcohol (PVA) was used as the stabilizer in the nanoprecipitation method. CFZ:PLGA ratios and PVA levels were considered as independent variables and mean Particle Size (PS), Polydispersity Index (PDI), Zeta Potential (ZP), and percent Entrapment Efficiency (EE) were chosen as the responses. Both the CFZ:PLGA ratio and PVA level were found to affect one or more responses. Furthermore, the optimized CFZ-PLGA-NPs had satisfactory PS, PDI, ZP, and EE respectively. In the next step the concentration of chitosan was evaluated for the formulation of C-CFZ-PLGA-NPs and a concentration of 0.25% was found to be optimum. The electron microscope images, FTIR spectra, and DSC thermograms confirmed the identity of individual components and the amorphous nature of CFZ in the C-CFZ-PLGA-NPs. The *in vitro* CFZ release from C-CFZ-PLGA-NPs was significantly higher than that from CFZ dispersion at 48 h. Cell line studies for the evaluation of cytotoxicity against liver cancer cells were carried out in HepG2 cells. The cell viability assay demonstrated significant enhancement of cytotoxicity of C-CFZ-PLGA-NPs against HepG2 cells compared to pure CFZ. The C-CFZ-PLGA-NPs were found to be stable when tested for storage stability at 4°C for 90 days. The study unveiled the effectiveness of C-CFZ-PLGA-NPs against pure CFZ in enhancing cytotoxicity. C-CFZ-PLGA-NPs can be considered potential candidates for further studies in providing a commercially viable, stable, and effective system for the delivery of CFZ.

REFERENCES

- Danhier F, Ansorena E, Silva JM, Coco R, Le Breton A, Pr at V. PLGA-based nanoparticles: an overview of biomedical applications. *J Control Release*. 2012;161(2):505-22. doi: 10.1016/j.jconrel.2012.01.043, PMID 22353619.
- Zhang D, Liu L, Wang J, Zhang H, Zhang Z, Xing G, *et al.* Drug-loaded PEG-PLGA nanoparticles for cancer treatment. *Front Pharmacol*. 2022;13:990505. doi: 10.3389/fphar.2022.990505, PMID 36059964.
- Lim YW, Tan WS, Ho KL, Mariatulqabtiyah AR, Abu Kasim NH, Abd Rahman N, *et al.* Challenges and complications of poly(lactic-co-glycolic acid)-based long-acting drug product development. *Pharmaceutics*. 2022;14(3):614. doi: 10.3390/pharmaceutics14030614, PMID 35335988.
- Dandamudi M, McLoughlin P, Behl G, Rani S, Coffey L, Chauhan A, *et al.* Chitosan-coated PLGA nanoparticles encapsulating triamcinolone acetonide as a potential candidate for sustained ocular drug delivery. *Pharmaceutics*. 2021;13(10):1590. doi: 10.3390/pharmaceutics13101590, PMID 34683883.
- Frank LA, Onzi GR, Morawski AS, Pohlmann AR, Guterres SS, Contri RV. Chitosan as a coating material for nanoparticles intended for biomedical applications. *React Funct Polym*. 2020;147:104459. doi: 10.1016/j.reactfunctpolym.2019.104459.
- Narmani A, Jafari SM. Chitosan-based nanodelivery systems for cancer therapy: recent advances. *Carbohydr Polym*. 2021;272:118464. doi: 10.1016/j.carbpol.2021.118464, PMID 34420724.
- Plosker GL. Canagliflozin: a review of its use in patients with type 2 diabetes mellitus. *Drugs*. 2014;74(7):807-24. doi: 10.1007/s40265-014-0225-5, PMID 24831734.
- Basak D, Gamez D, Deb S. SGLT2 Inhibitors as potential anticancer agents. *Biomedicines*. 2023;11(7):1867. doi: 10.3390/biomedicines11071867, PMID 37509506.
- Villani LA, Smith BK, Marcinko K, Ford RJ, Broadfield LA, Green AE, *et al.* The diabetes medication canagliflozin reduces cancer cell proliferation by inhibiting mitochondrial complex-I supported respiration. *Mol Metab*. 2016;5(10):1048-56. doi: 10.1016/j.molmet.2016.08.014, PMID 27689018.
- Ali A, Mekhael B, Biziotis OD, Tsakiridis EE, Ahmadi E, Wu J, *et al.* The SGLT2 inhibitor canagliflozin suppresses growth and enhances prostate cancer response to radiotherapy. *Commun Biol*. 2023;6(1):919. doi: 10.1038/s42003-023-05289-w, PMID 37684337.
- Ding L, Chen X, Zhang W, Dai X, Guo H, Pan X, *et al.* Canagliflozin primes antitumor immunity by triggering PD-L1 degradation in endocytic recycling. *J Clin Invest*. 2023;133(1):e154754. doi: 10.1172/JCI154754, PMID 36594471.
- Papadopoli D, Uchenunu O, Palia R, Chekkal N, Hulea L, Topisirovic I, *et al.* Perturbations of cancer cell metabolism by the antidiabetic drug canagliflozin. *Neoplasia*. 2021;23(4):391-9. doi: 10.1016/j.neo.2021.02.003, PMID 33784591.
- Kaji K, Nishimura N, Seki K, Sato S, Saikawa S, Nakanishi K, *et al.* Sodium glucose cotransporter 2 inhibitor canagliflozin attenuates liver cancer cell growth and angiogenic activity by inhibiting glucose uptake. *Int J Cancer*. 2018;142(8):1712-22. doi: 10.1002/ijc.31193, PMID 29205334.
- Hung MH, Chen YL, Chen LJ, Chu PY, Hsieh FS, Tsai MH, *et al.* Canagliflozin inhibits growth of hepatocellular carcinoma via blocking glucose-influx-induced β -catenin activation. *Cell Death Dis*. 2019;10(6):420. doi: 10.1038/s41419-019-1646-6, PMID 31142735.
- Wu H, Wang MD, Liang L, Xing H, Zhang CW, Shen F, *et al.* Nanotechnology for hepatocellular carcinoma: from surveillance, diagnosis to management. *Small*. 2021;17(6):e2005236. doi: 10.1002/sml.202005236, PMID 33448111.
- Sun R, Fang L, Lv X, Fang J, Wang Y, Chen D, *et al.* *In vitro* and *in vivo* evaluation of self-assembled chitosan nanoparticles selectively overcoming hepatocellular carcinoma via asialoglycoprotein receptor. *Drug Deliv*. 2021;28(1):2071-84. doi: 10.1080/10717544.2021.1983077, PMID 34595970.
- Ansari MJ, Alshahrani SM. Nano-encapsulation and characterization of baricitinib using poly-lactic-glycolic acid co-polymer. *Saudi Pharm J*. 2019;27(4):491-501. doi: 10.1016/j.jsps.2019.01.012, PMID 31061617.
- Orlewski PM, Ahn B, Mazzotti M. Tuning the particle sizes in spherical agglomeration. *Cryst Growth Des*. 2018;18(10):6257-65. doi: 10.1021/acs.cgd.8b01134.
- Alshamsan A. Nanoprecipitation is more efficient than emulsion solvent evaporation method to encapsulate cucurbitacin I in PLGA nanoparticles. *Saudi Pharm J*. 2014;22(3):219-22. doi: 10.1016/j.jsps.2013.12.002, PMID 25061407.
- Huang W, Zhang C. Tuning the size of poly(lactic-co-glycolic acid) (PLGA) nanoparticles fabricated by nanoprecipitation. *Biotechnol J*. 2018;13(1). doi: 10.1002/biot.201700203, PMID 28941234.
- Abrar I, Bhaskarwar AN. Effect of alcohols on water solubilization in surfactant-free diesel microemulsions. *Energy Rep*. 2022;8:504-12. doi: 10.1016/j.egyr.2022.10.157.
- Gaur M, Maurya S, Akhtar MS, Yadav AB. Synthesis and evaluation of BSA-loaded PLGA-chitosan composite nanoparticles for the protein-based drug delivery system. *ACS Omega*. 2023;8(21):18751-9. doi: 10.1021/acsomega.3c00738, PMID 37273604.
- Sahoo SK, Panyam J, Prabha S, Labhasetwar V. Residual polyvinyl alcohol associated with poly (d,l-lactide-co-glycolide) nanoparticles affects their physical properties and cellular uptake. *J Control Release*. 2002;82(1):105-14. doi: 10.1016/S0168-3659(02)00127-X, PMID 12106981.
- Jain AK, Swarnakar NK, Godugu C, Singh RP, Jain S. The effect of the oral administration of polymeric nanoparticles on the efficacy and toxicity of tamoxifen. *Biomaterials*. 2011;32(2):503-15. doi: 10.1016/j.biomaterials.2010.09.037, PMID 20934747.

25. Chiesa E, Dorati R, Modena T, Conti B, Genta I. Multivariate analysis for the optimization of microfluidics-assisted nanoprecipitation method intended for the loading of small hydrophilic drugs into PLGA nanoparticles. *Int J Pharm.* 2018;536(1):165-77. doi: 10.1016/j.ijpharm.2017.11.044, PMID 29175645.
26. Roces CB, Christensen D, Perrie Y. Translating the fabrication of protein-loaded poly(lactic-co-glycolic acid) nanoparticles from bench to scale-independent production using microfluidics. *Drug Deliv Transl Res.* 2020;10(3):582-93. doi: 10.1007/s13346-019-00699-y, PMID 31919746.
27. Moayedi H, Asadi A, Moayedi F, Huat BB. Zeta potential of tropical soil in presence of polyvinyl alcohol. *Int J Electrochem Sci.* 2011;6(5):1294-306. doi: 10.1016/S1452-3981(23)15074-7.
28. Tefas LR, Tomuță I, Achim M, Vlase L. Development and optimization of quercetin-loaded PLGA nanoparticles by experimental design. *Clujul Med.* 2015;88(2):214-23. doi: 10.15386/cjmed-418, PMID 26528074.
29. Fang DL, Chen Y, Xu B, Ren K, He ZY, He LL, *et al.* Development of lipid-shell and polymer core nanoparticles with water-soluble solidoside for anti-cancer therapy. *Int J Mol Sci.* 2014;15(3):3373-88. doi: 10.3390/ijms15033373, PMID 24573250.
30. Kizilbey K. Optimization of rutin-loaded PLGA nanoparticles synthesized by single-emulsion solvent evaporation method. *ACS Omega.* 2019;4(1):555-62. doi: 10.1021/acsomega.8b02767.
31. Mohd Izham MN, Hussin Y, Aziz MN, Yeap SK, Rahman HS, Masarudin MJ, *et al.* Preparation and characterization of self nano-emulsifying drug delivery system loaded with citral and its antiproliferative effect on colorectal cells. *Nanomaterials (Basel, Switzerland).* 2019;9(7):1028. doi: 10.3390/nano9071028, PMID 31323842.
32. Guo C, Gemeinhart RA. Understanding the adsorption mechanism of chitosan onto poly(lactide-co-glycolide) particles. *Eur J Pharm Biopharm.* 2008;70(2):597-604. doi: 10.1016/j.ejpb.2008.06.008, PMID 18602994.
33. Kong FH, Ye QF, Miao XY, Liu X, Huang SQ, Xiong L, *et al.* Current status of sorafenib nanoparticle delivery systems in the treatment of hepatocellular carcinoma. *Theranostics.* 2021;11(11):5464-90. doi: 10.7150/thno.54822, PMID 33859758.
34. Lu B, Lv X, Le Y. Chitosan-modified PLGA nanoparticles for control-released drug delivery. *Polymers.* 2019;11(2):304. doi: 10.3390/polym11020304, PMID 30960288.
35. Abd El Hady WE, Mohamed EA, Soliman OA, El-Sabbagh HM. *In vitro-in vivo* evaluation of chitosan-PLGA nanoparticles for potentiated gastric retention and anti-ulcer activity of diosmin. *Int J Nanomedicine.* 2019;14:7191-213. doi: 10.2147/IJN.S213836, PMID 31564873.
36. Burkhande NS, Wankhade VP, Atram SC, Bobade NN, Pande SD. Development of co-crystallization technique to improve solubility of anti-diabetic drug. *Asian J Pharm Res Dev.* 2023; 11(4)(4 SE-Research Articles):30-5. doi: 10.22270/ajprd.v11i4.1282.
37. Gupta S, Pramanik AK, Kailath A, Mishra T, Guha A, Nayar S, *et al.* Composition dependent structural modulations in transparent poly(vinyl alcohol) hydrogels. *Colloids Surf B Biointerfaces.* 2009;74(1):186-90. doi: 10.1016/j.colsurfb.2009.07.015, PMID 19700267.
38. Jipa I, Stoica A, Stroescu M, Dobre LM, Dobre T, Jinga S, *et al.* Potassium sorbate release from poly(vinyl alcohol)-bacterial cellulose films. *Chemical Papers.* 2012;66(2):138-43. doi: 10.2478/s11696-011-0068-4. doi: 10.2478/s11696-011-0068-4.
39. Morsy M, Mostafa K, Aryn H, El-Ebissy AA, Salah AM, Youssef MA. Synthesis and Characterization of Freeze Dryer chitosan Nano particles as Multi functional Eco-Friendly Finish for Fabricating Easy Care and antibacterial Cotton Textiles. *Egypt J Chem.* 2019;62(7):1277-93. doi: 10.21608/ejchem.2019.6995.1583.
40. Patel NC, Patel HA. A recent solidification approach for nanosuspension: formulation, optimisation and evaluation of canagliflozin immediate release pellets. *Folia Med (Plovdiv).* 2022;64(3):488-500. doi: 10.3897/folmed.64.e68866, PMID 35856111.
41. Ayyoob M, Kim YJ. Effect of chemical composition variant and oxygen plasma treatments on the wettability of PLGA thin films, synthesized by direct Copolycondensation. *Polymers (Basel).* 2018;10(10):1132. doi: 10.3390/polym10101132, PMID 30961057.
42. Zhang Z, Wang X, Zhu R, Wang Y, Li B, Ma Y, *et al.* Synthesis and characterization of serial random and block-copolymers based on lactide and glycolide. *Polym Sci Ser B.* 2016;58(6):720-9. doi: 10.1134/S1560090416060191.
43. Gupta S, Pramanik AK, Kailath A, Mishra T, Guha A, Nayar S, *et al.* Composition dependent structural modulations in transparent poly(vinyl alcohol) hydrogels. *Colloids Surf B Biointerfaces.* 2009;74(1):186-90. doi: 10.1016/j.colsurfb.2009.07.015, PMID 19700267.
44. Rahman L, Goswami J, Choudhury D. Assessment of physical and thermal behaviour of chitosan-based biocomposites reinforced with leaf and stem extract of *Tectona grandis*. *Polym Polym Compos.* 2022; 30. doi: 10.1177/09673911221076305.
45. Dandamudi M, McLoughlin P, Behl G, Rani S, Coffey L, Chauhan A, *et al.* Chitosan-coated PLGA nanoparticles encapsulating triamcinolone acetonide as a potential candidate for sustained ocular drug delivery. *Pharmaceutics.* 2021;13(10):1590. doi: 10.3390/pharmaceutics13101590, PMID 34683883.
46. Fong SS, Foo YY, Saw WS, Leo BF, Teo YY, Chung I, *et al.* Chitosan-coated-PLGA nanoparticles enhance the antitumor and antimigration activity of Stattic – a STAT3 dimerization blocker. *Int J Nanomedicine.* 2022;17:137-50. doi: 10.2147/IJN.S337093, PMID 35046650.
47. López-García J, Lehocný M, Humpolíček P, Sába P. HaCaT keratinocytes response on antimicrobial atelocollagen substrates: extent of cytotoxicity, cell viability and proliferation. *J Funct Biomater.* 2014;5(2):43-57. doi: 10.3390/jfb5020043, PMID 24956439.
48. Findlay RD, Tausch HW, David-Cu R, Walther FJ. Lysis of red blood cells and alveolar epithelial toxicity by therapeutic pulmonary surfactants. *Pediatr Res.* 1995;37(1):26-30. doi: 10.1203/00006450-199501000-00006, PMID 7700730.
49. Angelopoulou A, Kolokithas-Ntoukas A, Papaioannou L, Kakazanis Z, Khoury N, Zoumpourlis V, *et al.* Canagliflozin-loaded magnetic nanoparticles as potential treatment of hypoxic tumors in combination with radiotherapy. *Nanomedicine (Lond).* 2018;13(19):2435-54. doi: 10.22217/nnm-2018-0145, PMID 30311542.
50. Alshememry A, Kalam MA, Almoghrabi A, Alzahrani A, Shahid M, Khan AA, *et al.* Chitosan-coated poly (lactic-co-glycolide) nanoparticles for dual delivery of doxorubicin and naringin against MCF-7 cells. *J Drug Deliv Sci Technol.* 2022;68:103036. doi: 10.1016/j.jddst.2021.103036.
51. Carone A, Emilsson S, Mariani P, Désert A, Parola S. Gold nanoparticle shape dependence of colloidal stability domains. *Nanoscale Adv.* 2023;5(7):2017-26. doi: 10.1039/D2NA00809B, PMID 36998666.

Cite this article: Shadab Md, Alharthi EAA, Karim S. Development and Evaluation of Chitosan-Coated PLGA Nanoparticles of Canagliflozin for the Treatment of Hepatic Cancer. *Indian J of Pharmaceutical Education and Research.* 2026;60(2s):s475-s489.